# Amplitude-encoding FWI using different bases

He Liu, Daniel Trad and Kris Innanen

Dec 3rd, 2021

NSERC CRSNG
UNIVERSITY OF CALGARY
FACULTY OF SCIENCE
Department of Geoscience

# Outline

- Motivation
- Amplitude-encoding strategy
- Results for acoustic FWI
- Results for elastic FWI
- Conclusions

# Motivation

***Sources***

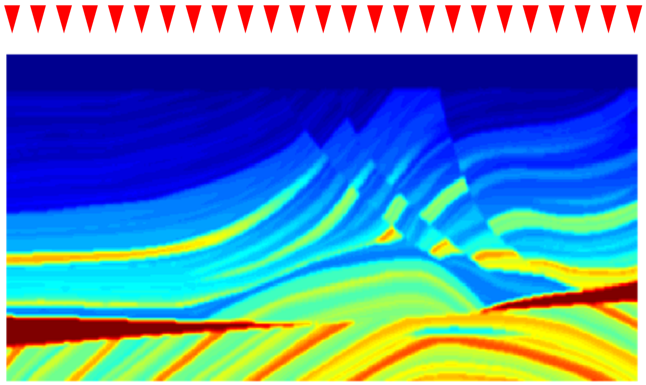

Model

Individual shot

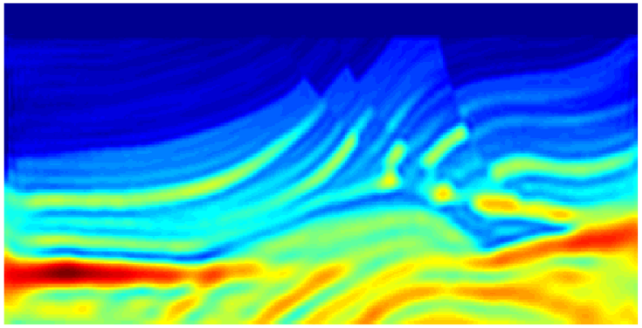

FWI image

# Motivation

To reduce the costs of both data acquisition and processing, source-encoding strategies have been used to perform FWI, which achieve better efficiency by the reduction of data dimension.

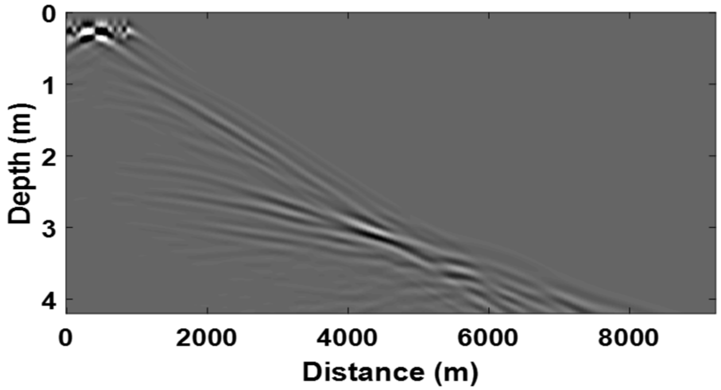


Random polarity encoding modifies the phase of the shot gathers.

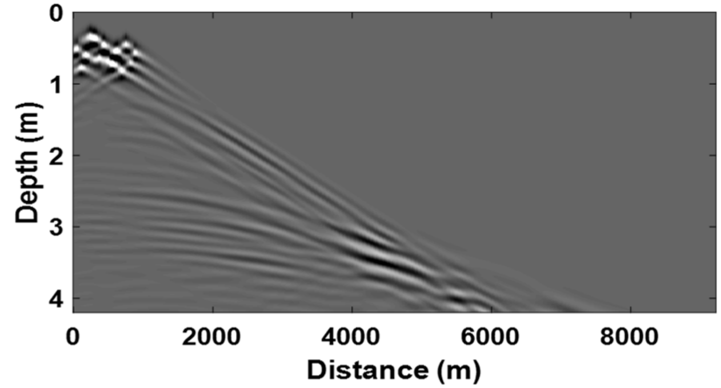


Random time delay encoding usually requires zero-padding the input shot gathers along the time axis.

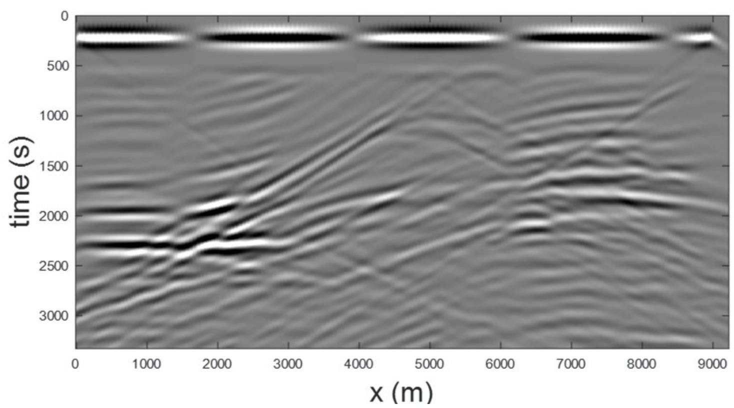


The amplitude encoding scheme is performed by applying different amplitude weights to the shot gathers or source wavelets.
One super-shot contains all the shot gathers.

# Acoustic FWI in time domain

The objective function (data misfit function) taking the l2-norm of the misfit vector $\delta p$ is given by

$$E(m) = \frac{1}{2}\delta p^{\dagger}\delta p = \frac{1}{2}\| p_{cal} - p_{obs} \|^2 \quad (1)$$

where † denotes the adjoint operator (conjugate transpose).

In encoding FWI, shot gathers are transformed into super-shots by the encoding matrix, which is defined as

$$\mathbf{B} = \begin{bmatrix} b^{1,1} & b^{2,1} & . & b^{N_{ig},1} \\ b^{1,2} & b^{2,2} & . & b^{N_{sig},2} \\ . & . & . & . \\ b^{1,N_{sup}} & b^{2,N_{sup}} & . & b^{N_{sig}\cdot N_{sup}} \end{bmatrix}_{Nsup\times Nsig} \quad (2)$$

where *Nsup* is the number of the super-shots and *Nsig* is the number of the individual shots (*Nsup* < *Nsig*).

The *Nsig* synthetic data and observed data are blended into *Nsup* blended data by

$$\begin{aligned} p^{\text{sup}}_{\text{cal}\ Nsup\times nt\times nr} &= \mathbf{B}p_{\text{cal}\ Nsig\times nt\times nr} \\ p^{\text{sup}}_{\text{obs}\ Nsup\times nt\times nr} &= \mathbf{B}p_{\text{obs}\ Nsig\times nt\times nr} \end{aligned} \quad (3)$$

# Acoustic FWI using blended data

Then we define the objective function of encoding FWI in a l-2 norm sense by:

$$E(\mathbf{m}) = \frac{1}{2}\left\|p_{cal}^{sup} - p_{obs}^{sup}\right\|^2 = \frac{1}{2}\left\|\mathbf{B}p_{cal} - \mathbf{B}p_{obs}\right\|^2 \qquad (5)$$
$$= \frac{1}{2}\left(p_{cal} - p_{obs}\right)\boxed{\mathbf{B}^T\mathbf{B}}\left(p_{cal} - p_{obs}\right)$$

The Hartley encoding matrix is defined as (Tsitsas et al., 2010):

$$\mathbf{b}_{m,n} = \cos\left(\frac{2\pi mn}{n_{\mathrm{sig}}}\right) + \sin\left(\frac{2\pi mn}{n_{\mathrm{sig}}}\right)$$

The discrete form of the cosine basis is (Hu et al., 2010) :

$$\mathbf{b}_{m,n} = \sqrt{\frac{2}{n_{\mathrm{sig}}}}\cos\left(\frac{\pi}{n_{\mathrm{sig}}}\frac{(2m\%n_{\mathrm{sig}}+1)(2n+1)}{4}\right)$$

The sine basis is defined as (Tsitsas et al., 2010) :

$$\mathbf{b}_{m,n} = \sqrt{\frac{2}{n_{\mathrm{sig}}}}\sin\left(\frac{\left(m+\frac{1}{2}\right)\left(n+\frac{1}{2}\right)\pi}{n_{\mathrm{sig}}}\right)$$

The random polarity basis (Krebs et al., 2010) :

$$\mathbf{b}_{m,n} = 1 \text{ or } -1$$

where *m* = 1,…, Nsig is the shot-index, *n* = 1,…, Nsup is the super-shot index, and *nsig* is the periodization index, % is the remainder operator.

# Model & Geometry

- Seismic survey geometry: 140 sources and 576 receivers.

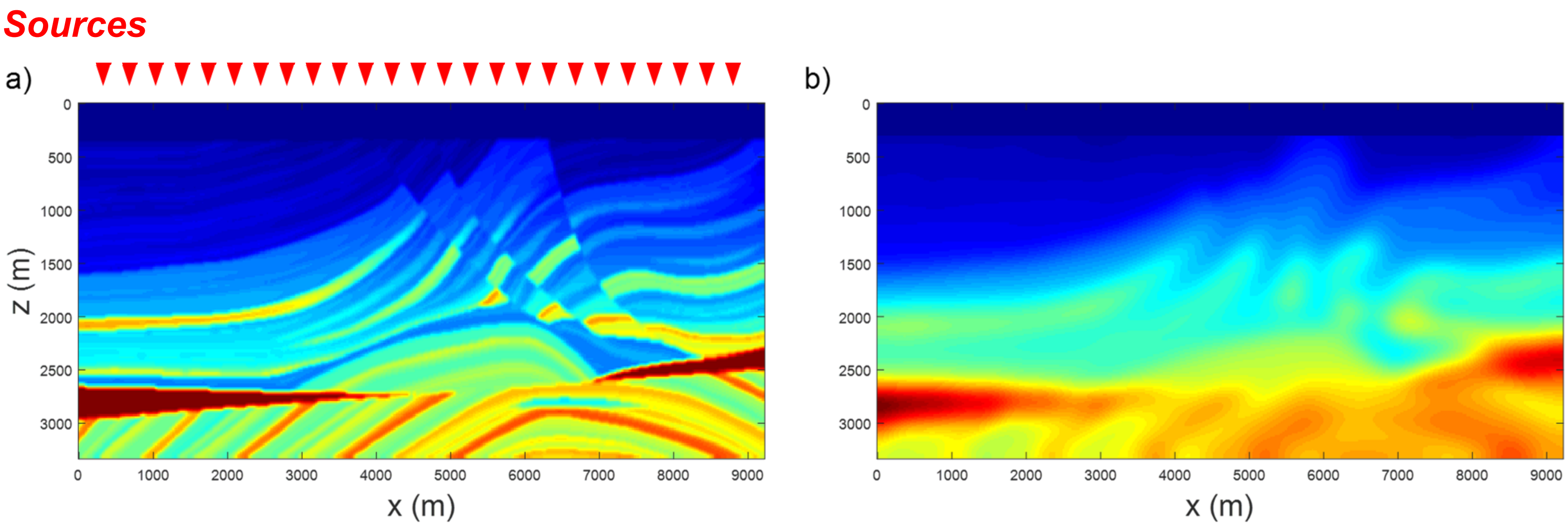


Fig 1. (a) The original Marmousi model. (b) The initial model.

We used Marmousi model and simulated 140 shots with 64-m interval.
We recorded 4.2 s of seismic data with 576 receivers.

# Encoding matrices

We use different bases as encoding functions. For comparison, we blend all the shot gathers into **7**, **35** and **70** super-shots.

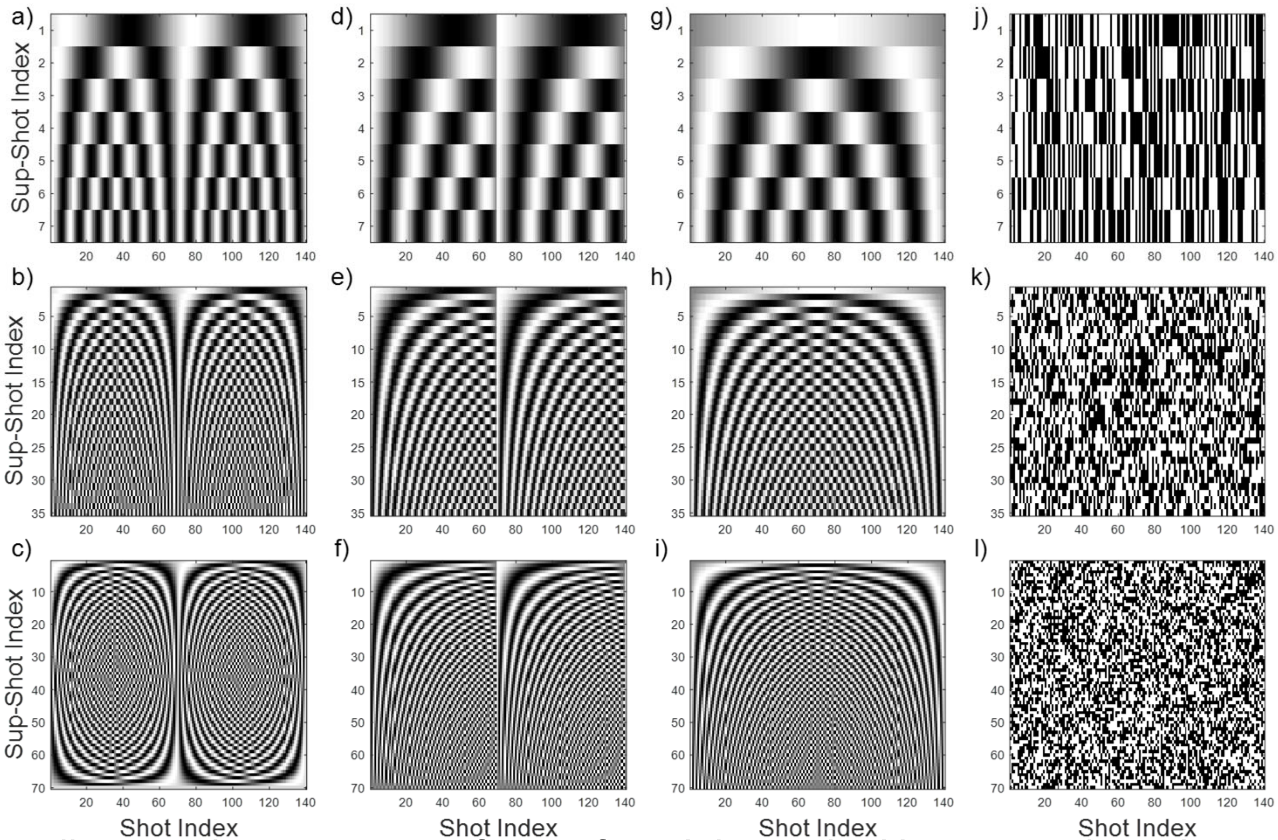


Fig .Amplitude encoding matrices: columns from left to right are by Hartley, cosine, sine and random polarity bases; rows from up to down are for 7, 35 and 70 super-shots, respectively.

# Crosstalk matrices

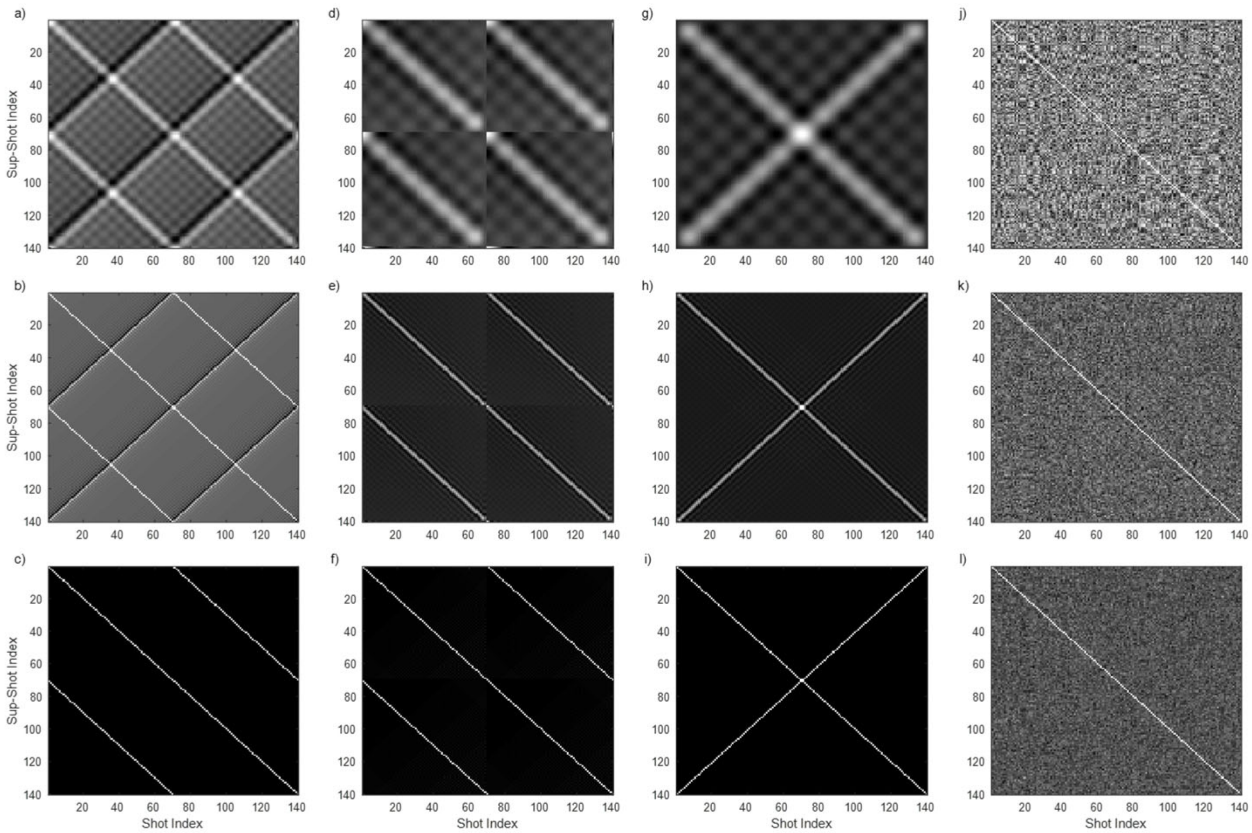


Fig. Crosstalk matrices: columns from left to right are by Hartley, cosine, sine and random polarity bases; rows from up to down are for 7, 35 and 70 super-shots, respectively.

# Synthetic shots

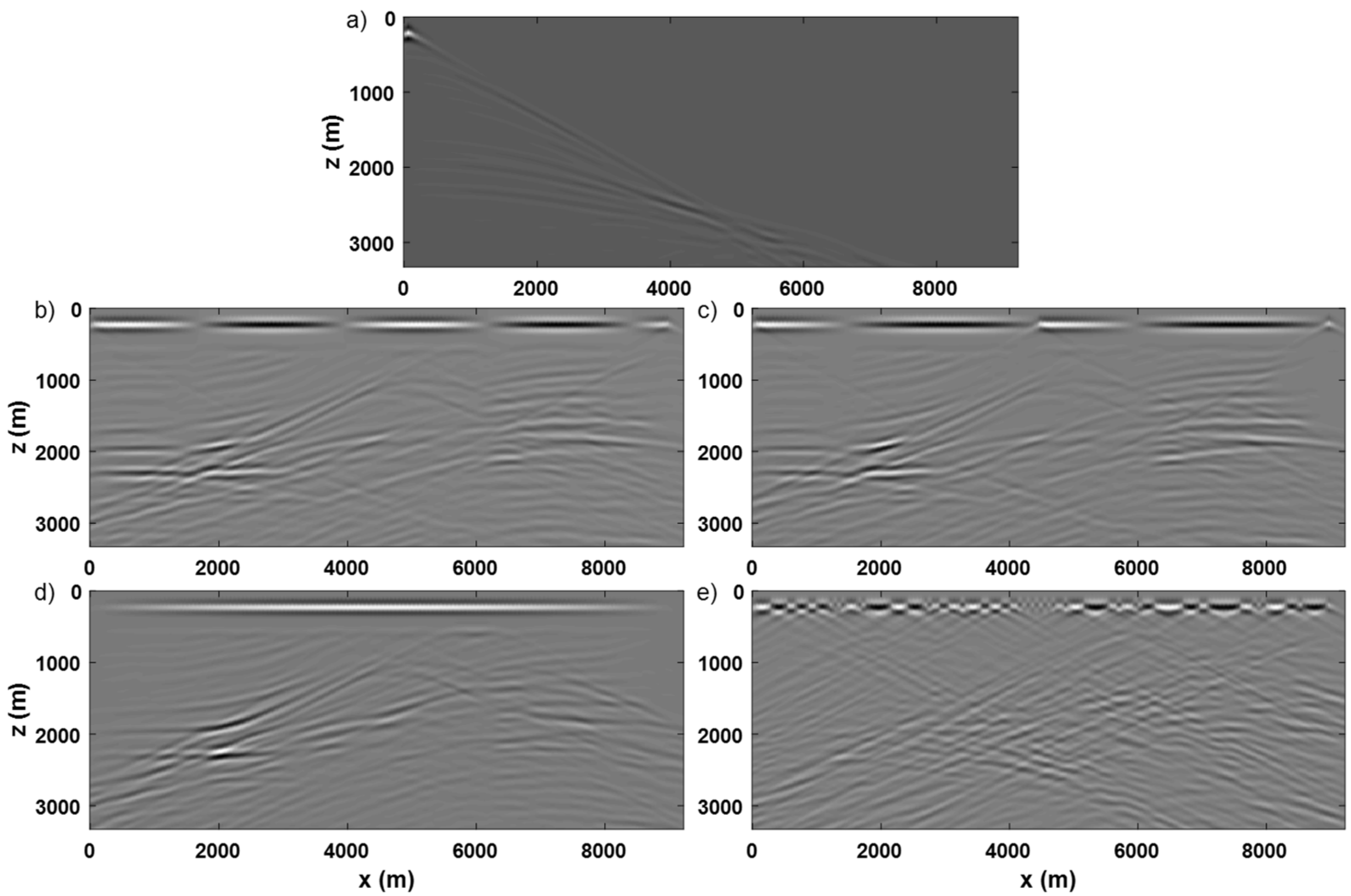


Fig. a) is the first individual shot in the conventional case; b) to e) are the first super-shot in the amplitude-encoding cases.

# Inversion results

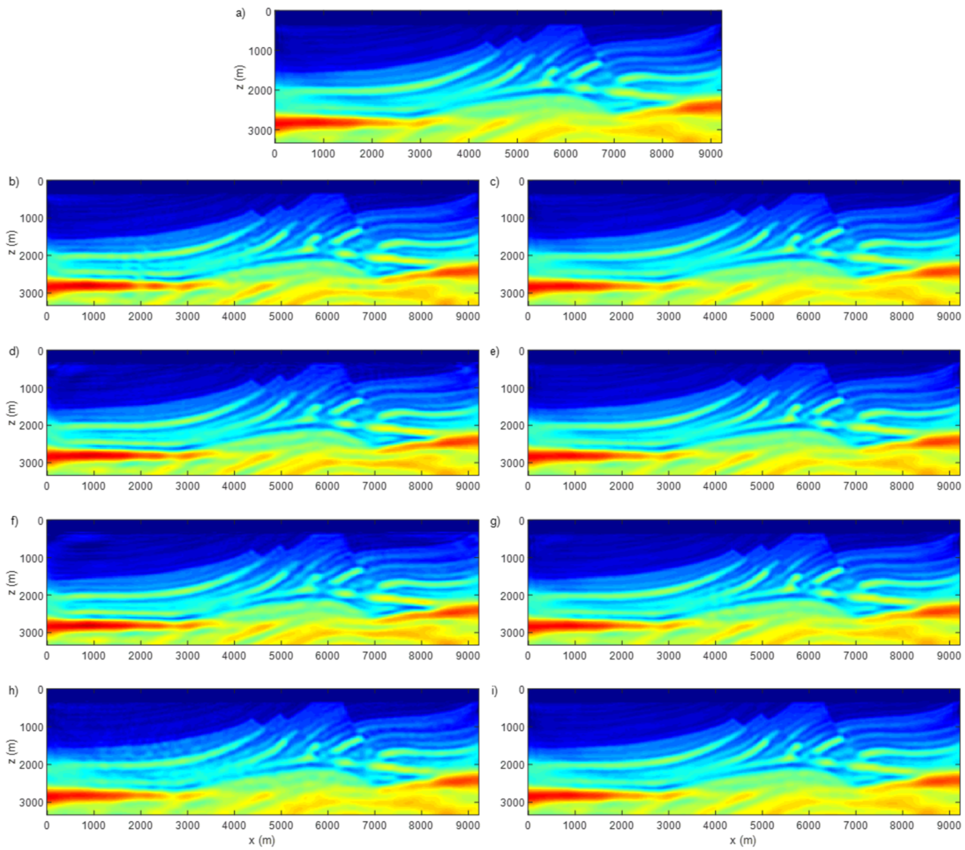


The updated velocity models after 25 iterations: a) by conventional FWI; b) and c) are by Hartley basis with 7 and 70 super-shots; d) and e) are by cosine basis with 7 and 70 super-shots; f) and g) are by sine basis with 7 and 70 super-shots; h) and i) are by random polarity basis with 7 and 70 super-shots.

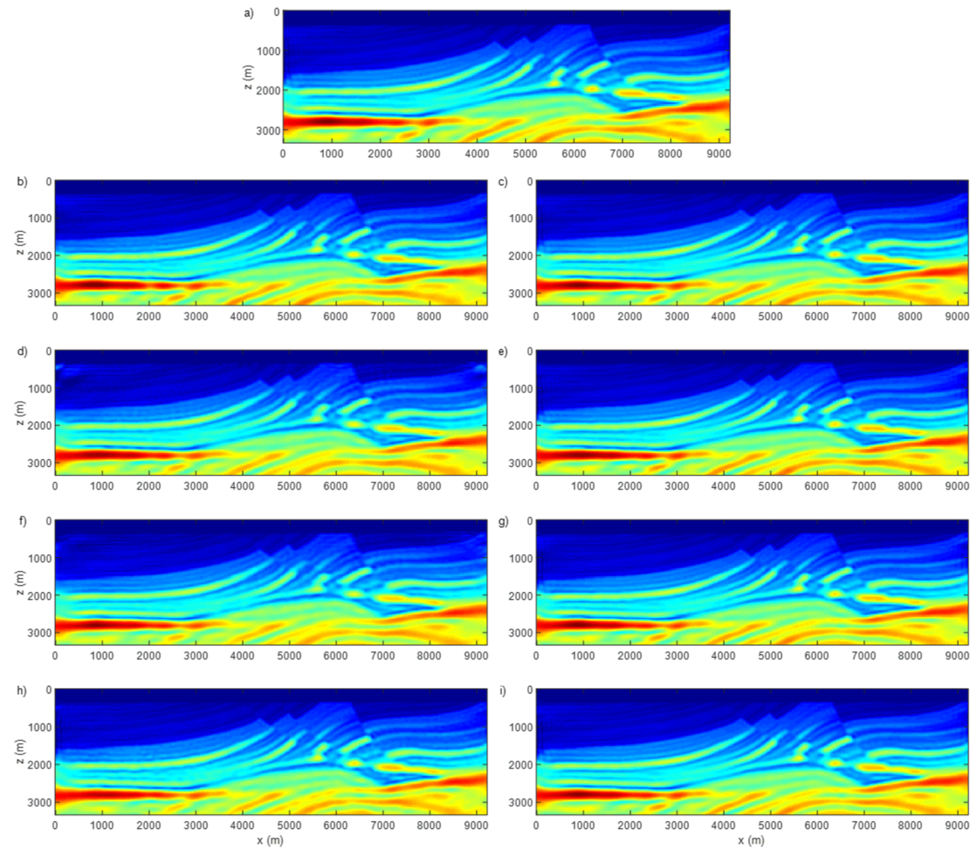


The updated velocity models after 100 iterations: a) by conventional FWI; b) and c) are by Hartley basis with 7 and 70 super-shots; d) and e) are by cosine basis with 7 and 70 super-shots; f) and g) are by sine basis with 7 and 70 super-shots; h) and i) are by random polarity basis with 7 and 70 super-shots.

# Data misfit

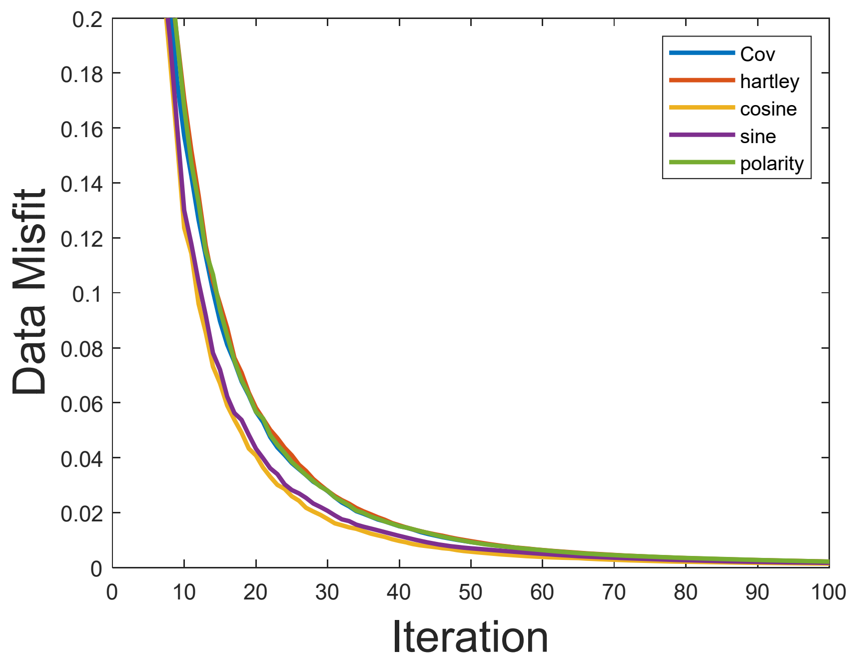


Fig. Comparison of data misfit function versus iteration

Dynamic encoding (Krebs et al., 2009) :

Instead of changing the encoding function, we dynamically reduce the number of super-shots every a few iterations to further reduce the data dimension.

70 super-shots → 35 super-shots →

14 super-shots → 7 super-shots

# Inversion results using dynamic-encoding concept

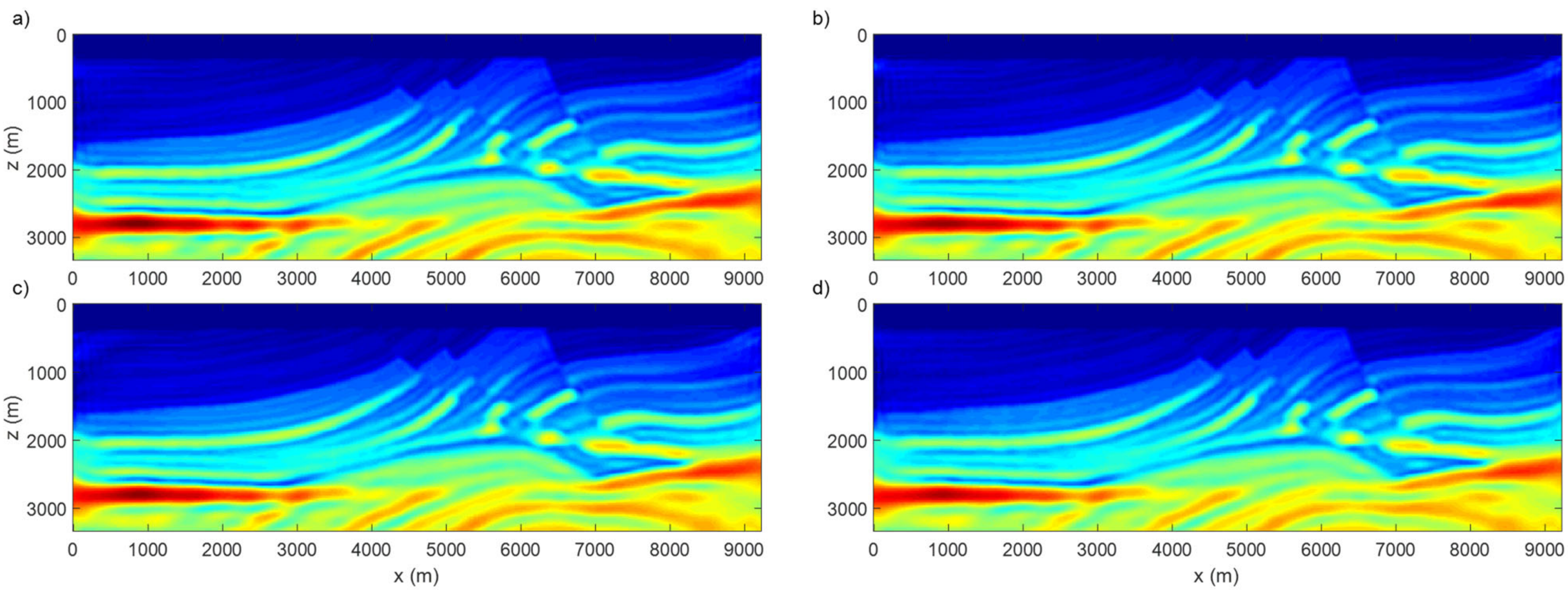


Fig. Inversions results using dynamic-encoding concept by different bases: a) Hartley; b) cosine; c) sine and d) random polarity.

# Amplitude-encoding FWI using dynamic encoding concept

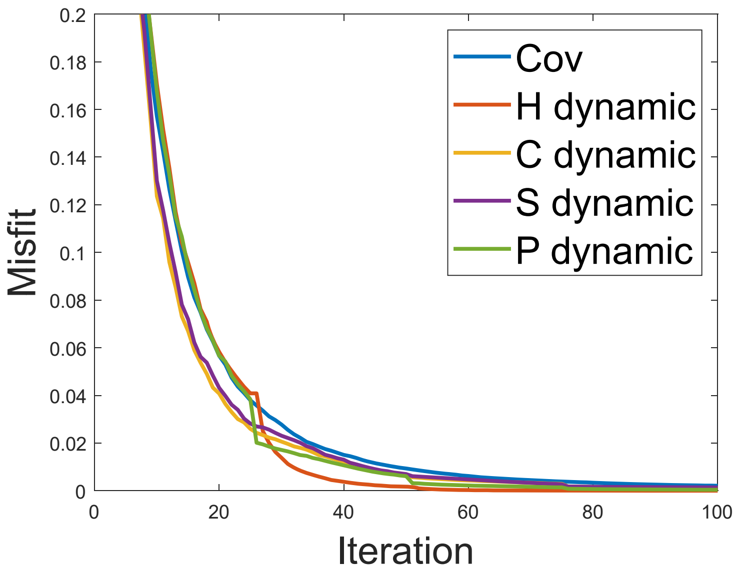


Fig. Comparison of misfit function versus iteration.

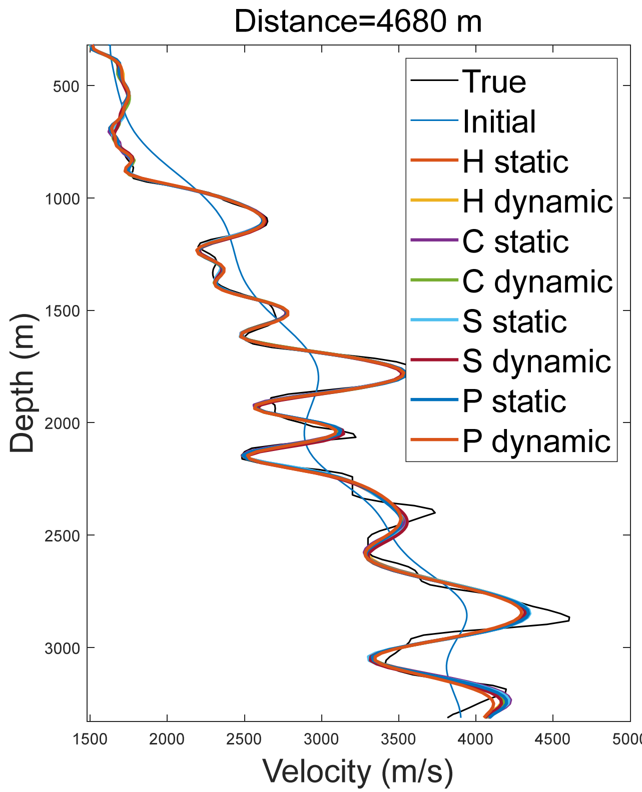


Fig. Comparison of vertical profiles in the middle of the model.

The number of super-shots is changed every 25 iterations, the data misfit curves may not be smooth.

# Results for foothill model

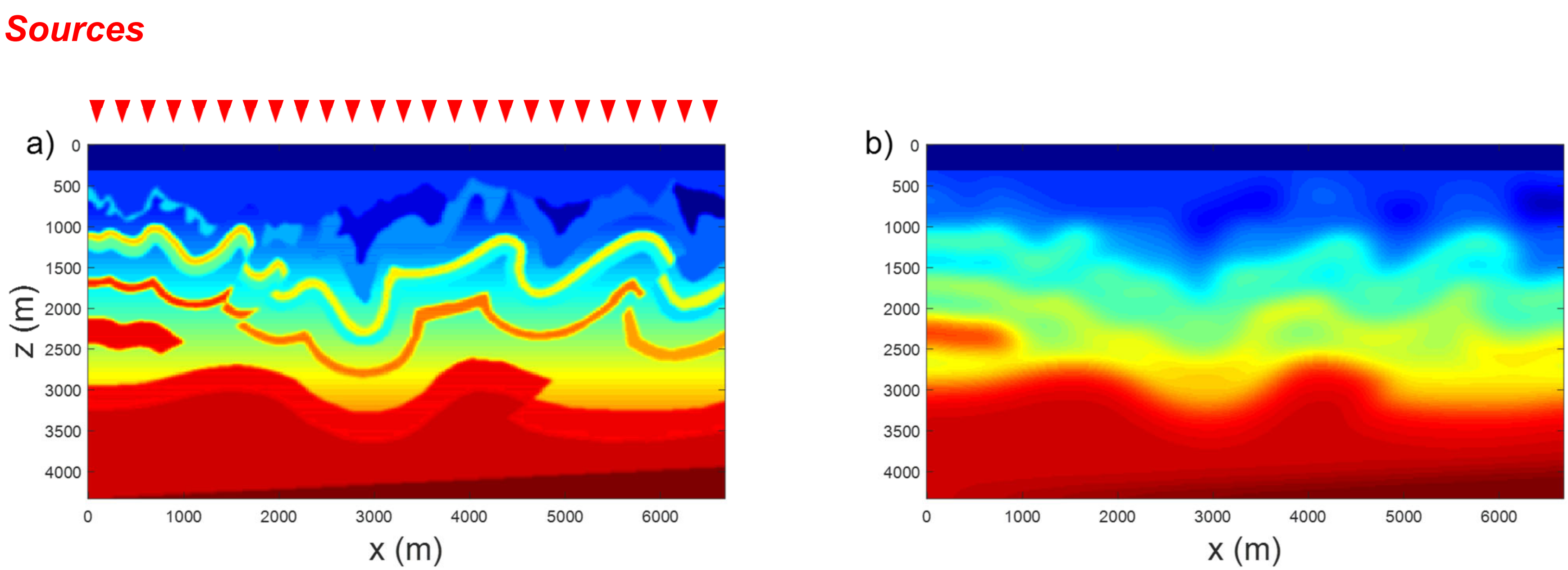


Fig. (a) The original model. (b) The initial model.

| | |
|---|---|
| Model size: | 250*417 |
| Number of sources: | 100 |
| Central frequency: | 8 Hz |
| Dx : | 16 m |

# Results for foothill model

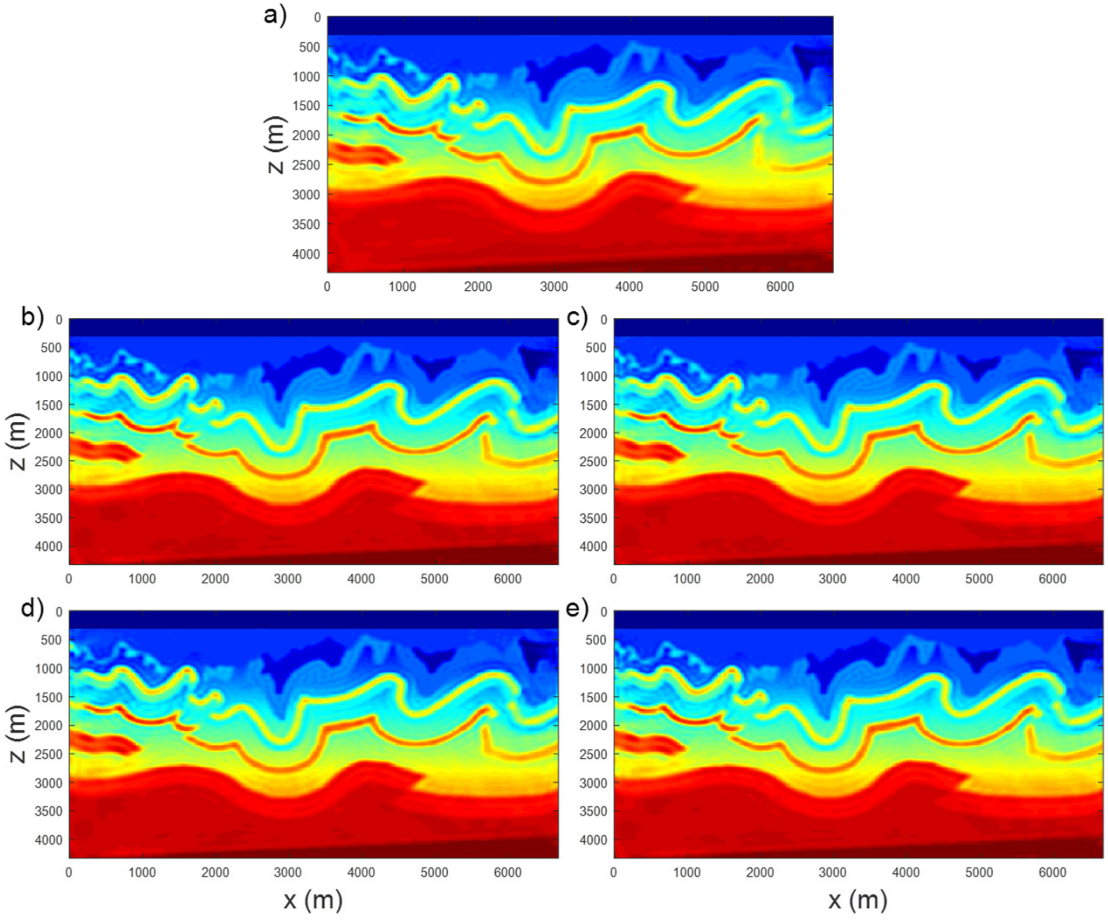


Fig. Dynamic inversion results: a) Conventional; b) Hartley; c) Cosine; d) Sine; e) Polarity.

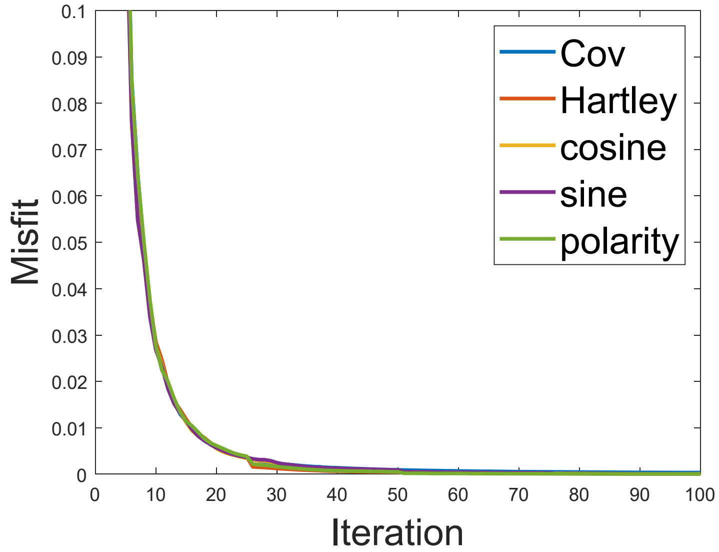


Fig. Comparison of misfit function versus iteration.

# Amplitude-encoding elastic FWI

In isotropic elastic media, the first-order stress-velocity wave equation can be rewritten as

$$\begin{cases} \rho \dfrac{\partial v_i}{\partial t} = \dfrac{\partial \sigma_{ij}}{\partial x_j} + f_i \\ \dfrac{\partial \sigma_{ij}}{\partial t} = \lambda \dfrac{\partial \theta}{\partial t} \delta_{ij} + 2\mu \dfrac{\partial \varepsilon_{ij}}{\partial t} \\ \dfrac{\partial \varepsilon_{ij}}{\partial t} = \dfrac{1}{2} \left( \dfrac{\partial v_i}{\partial x_j} + \dfrac{\partial v_j}{\partial x_i} \right) \end{cases}$$

where ρ is the density, σ is the stress, v is the velocity, λ and μ are Lame coefficients.

The objective function of encoding FWI in a l-2 norm sense is defined by:

$$\begin{aligned} E(\mathbf{m}) &= \frac{1}{2} \left\| p_{cal}^{sup} - p_{obs}^{sup} \right\|^2 = \frac{1}{2} \left\| \mathbf{B} p_{cal} - \mathbf{B} p_{obs} \right\|^2 \\ &= \frac{1}{2} \left( p_{cal} - p_{obs} \right) \boxed{\mathbf{B}^T \mathbf{B}} \left( p_{cal} - p_{obs} \right) \end{aligned}$$

In this work, we use the software IFOS2D to do the experiments.

# Marmousi II elastic model

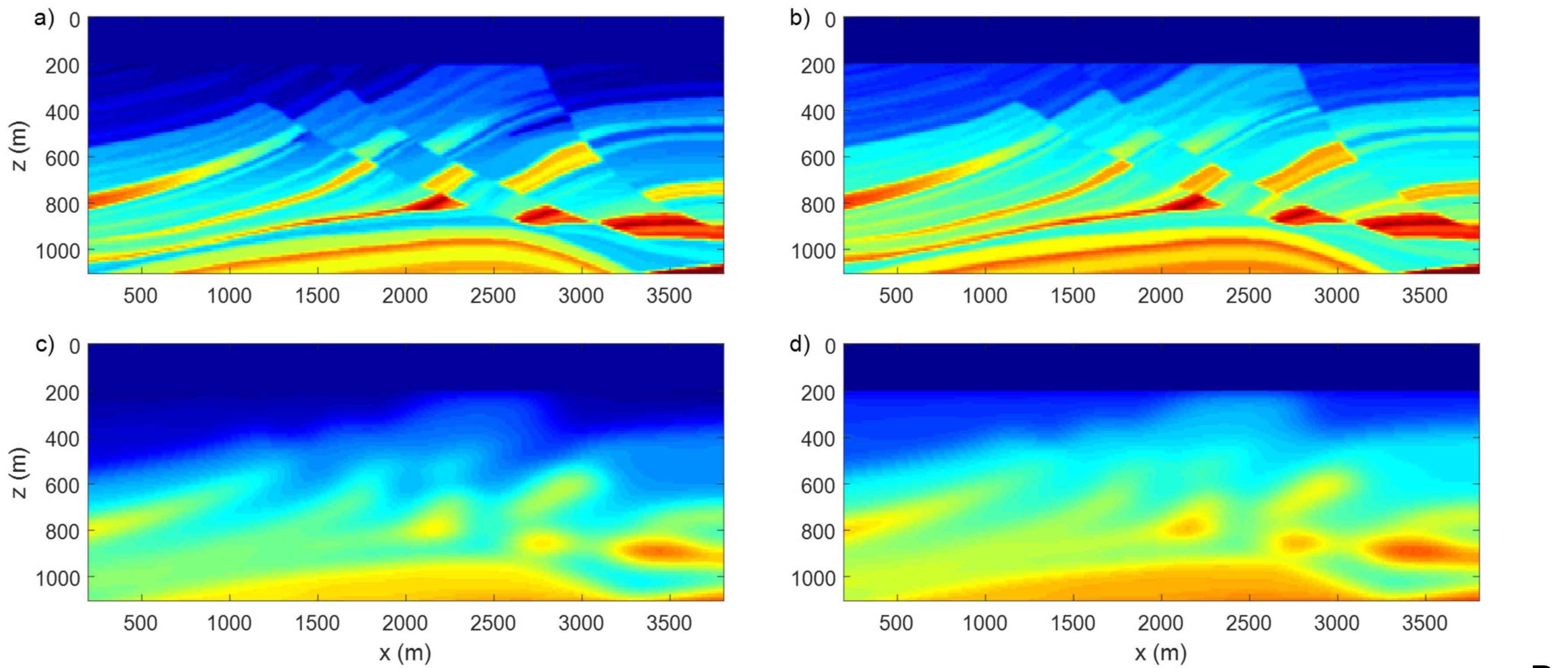


Fig. Subsampled Marmousi II model: a) and b) are true vp and vs; c) and d) are initial vp and vs.

We fire 40 explosive sources and use 360 two–component receivers to record the shots.

Parameters:
Dx: 10 m
Dt: 1 ms
T: 3.0 s
F: 10 hz

# Encoding and crosstalk matrices

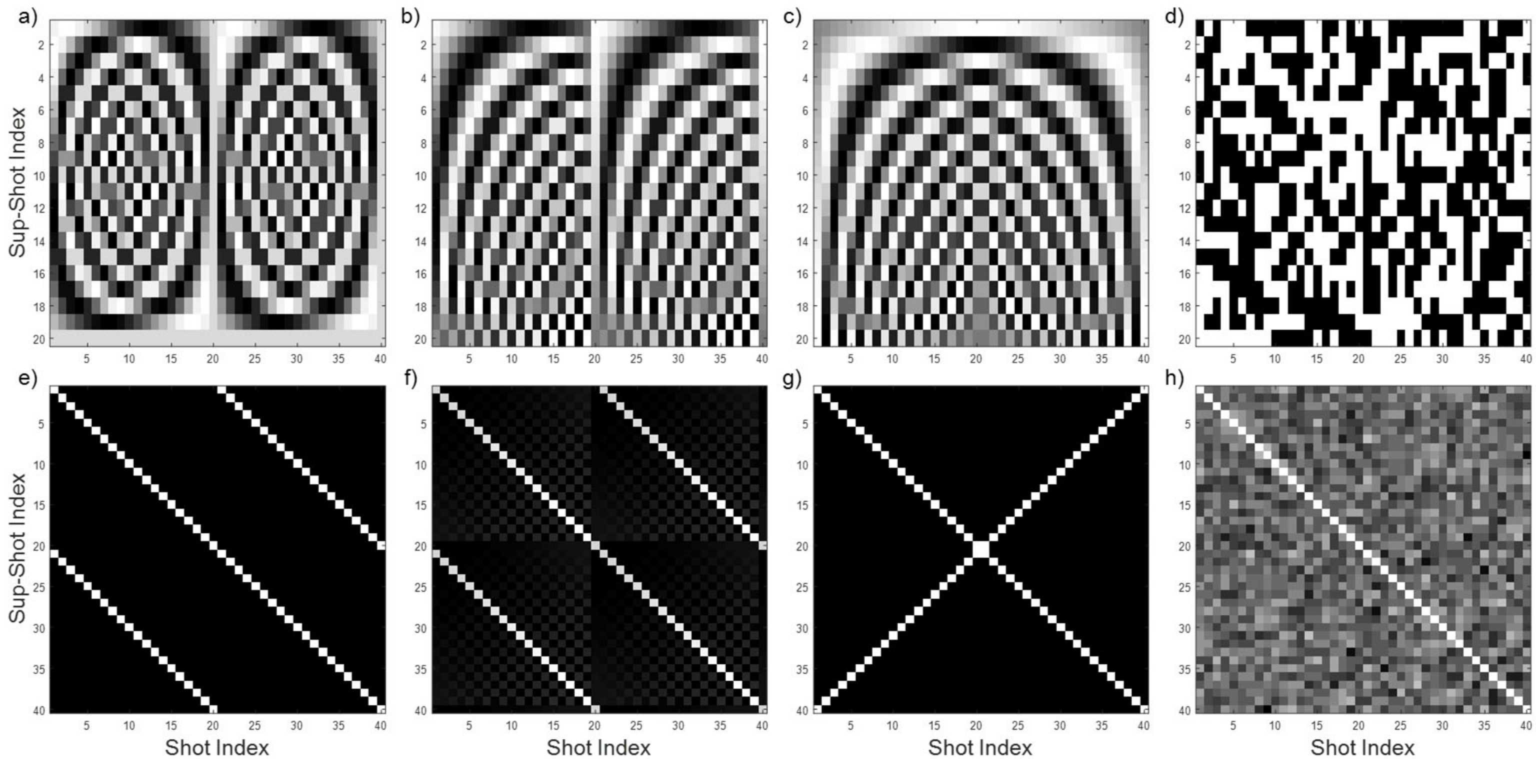


Fig. The amplitude encoding and corresponding crosstalk matrices: columns from left to right are for Hartley, cosine, sine and random polarity bases.

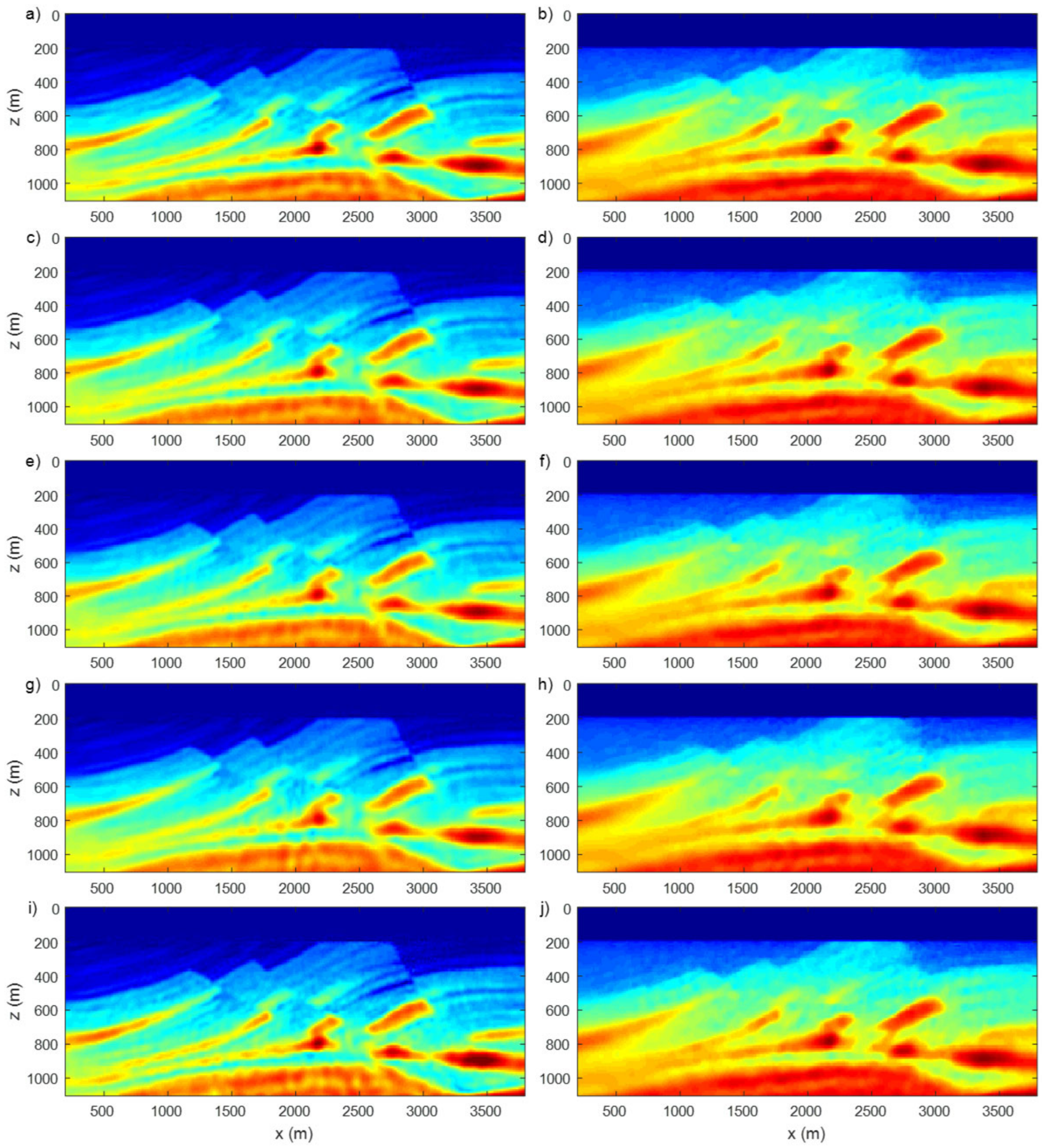


Fig. Inversion results by both conventional and amplitude-encoding FWI: left column is inverted vp, right column is inverted vs; from up to down are inverted parameters by conventional FWI, amplitude-encoding FWI using Hartley, cosine, sine and random polarity bases.

# Comparison of vertical profiles

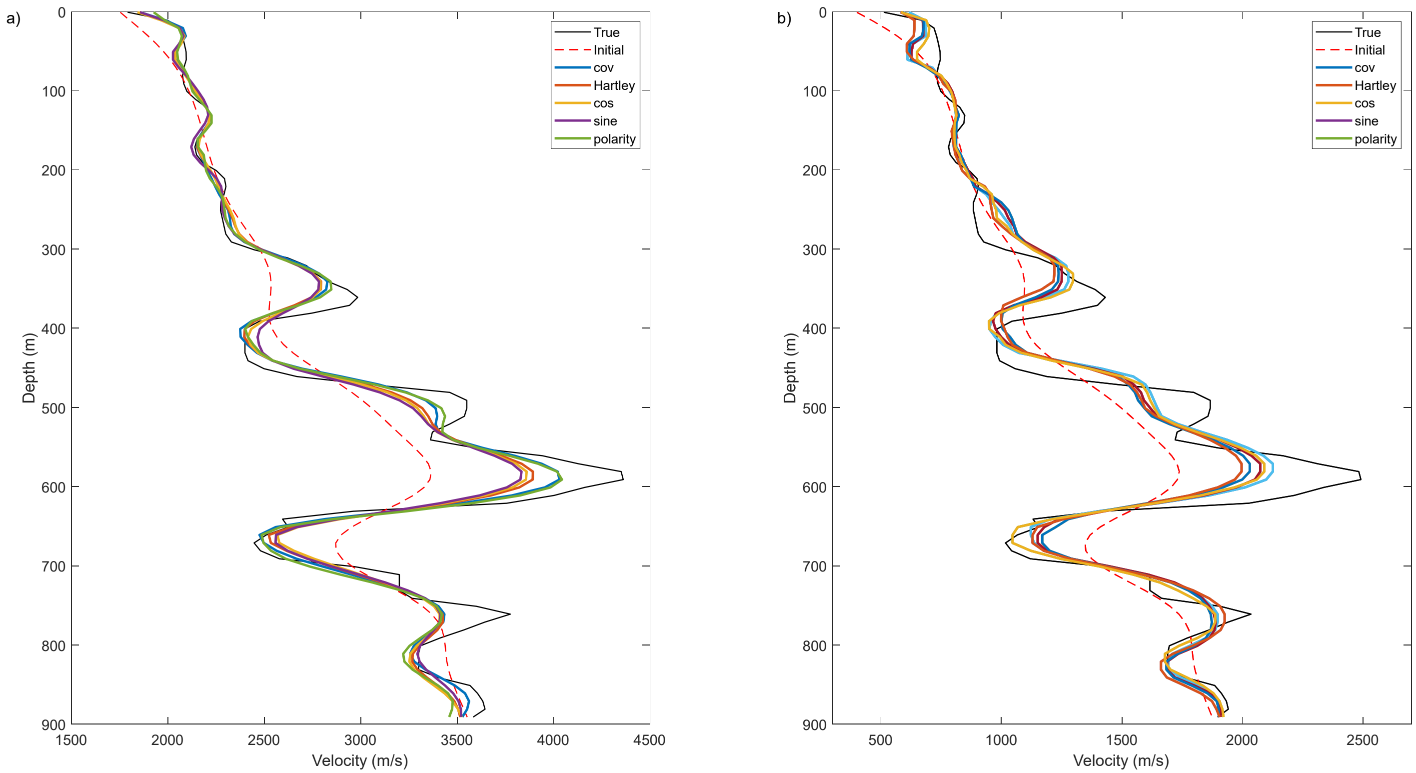


Fig. Depth profiles at distance 2.2 km of the initial model and inversion results are compared with the true model for the Marmousi II model: P-wave velocity (left), S-wave velocity (right).

# Conclusions

1. In this work, we present amplitude-encoding acoustic and elastic FWI using different bases as the encoding functions and compare their performance with conventional FWI.
2. We first use Marmousi model to show that amplitude-encoding acoustic FWI using different bases can mitigate the crosstalk noise very well and produce totally comparable inverted models and convergence rate to the conventional case. Then we demonstrate the feasibility of this strategy using a foothill model.
3. In addition, we adopt the dynamic-encoding concept and reduce the number of super-shots during the inversion process to further improve the calculation efficiency, producing almost the same updated velocity models as in the static-encoding cases.
4. We further apply amplitude-encoding strategy to elastic FWI and prove that this strategy also shows great performance for multi-parameter FWI.

# Acknowledgements


- CREWES sponsors, staff and students
- NSERC
- Dr. Pengliang Yang
- Developers of software IFOS2D

# References


Köhn, D. (2011). Time domain 2D elastic full waveform tomography (Doctoral dissertation).

Godwin, J., & Sava, P. (2013). A comparison of shot-encoding schemes for wave-equation migration. Geophysical Prospecting, 61, 391-408.

Hu, J., Wang, H., Fang, Z., Li, T., and Zhang, J., 2016, Efficient amplitude encoding least-squares reverse time migration using cosine basis: Geophysical prospecting, **64**, No. 6, 1483–1497.

Krebs, J. R., Anderson, J. E., Hinkley, D., Neelamani, R., Lee, S., Baumstein, A., & Lacasse, M. D. (2009). Fast full-wavefield seismic inversion using encoded sources. Geophysics, 74(6), WCC177-WCC188.

Romero L A, et al. Phase encoding of shot records in prestack migration[J]. Geophysics, 2000, 65(2): 426-436.

Tsitsas N L. On block matrices associated with discrete trigonometric transforms and their use in the theory of wave propagation[J]. Journal of Computational Mathematics, 2010: 864-878.